AIAA JOURNAL
Vol. 38, No. 3, March 2000

Resonance in Axisymmetric Jet Under Controlled Helical, Fundamental, and Axisymmetric Subharmonic Forcing

Sung Kwon Cho,* Jung Yul Yoo,† and Haecheon Choi‡
Seoul National University, Seoul 151-742, Republic of Korea

An axisymmetric jet is forced with two helical fundamental waves of identical frequency spinning in the opposite directions and an additional axisymmetric subharmonic wave. The subharmonic component rapidly grows downstream from resonant interaction with the fundamental, significantly depending on the initial phase difference between the subharmonic and the fundamental. The variation of the subharmonic amplitude with the initial phase difference shows a cusplike shape. The amplification of the subharmonic results in a vortex pairing of helical modes. Furthermore, the azimuthal variation of the amplification induces an asymmetric jet cross section. When the initial subharmonic is imposed with an initial phase difference close to a critical value, the jet cross section evolves into a three-lobed shape. The lobes are generated by vortex pairing. Therefore, the conclusion is made that the initial phase difference between the fundamental and the subharmonic plays an important role in controlling the jet cross section.

Nomenclature

a_s = subharmonic amplitude at jet exit $[(u'_s/U_e)|_{x=0}]$
D = jet diameter
f = fundamental frequency
m = azimuthal wave number
p = sound pressure
Re_D = Reynolds number based on jet diameter $(U_e D/\nu)$
r = radial coordinate
$r_{0.1}$ = radial position, where $U/U_c = 0.1$
Sr_D = Strouhal number based on jet diameter (fD/U_e)
U = streamwise mean velocity
u = streamwise velocity fluctuation
x = streamwise coordinate
γ = azimuthal angle
θ = momentum thickness:

$$\left(\int_0^{r_{0.1}} \frac{U}{U_c}\left(1-\frac{U}{U_c}\right)\mathrm{d}r\right)$$

ν = kinematic viscosity
ϕ_d = local phase difference between the fundamental and the subharmonic $(\phi_f - 2\phi_s)$
ϕ_{de} = initial phase difference between the helical fundamental mode pair and the axisymmetric subharmonic measured at $x/D = 0$, $r/D = 0.25$, and $\gamma = 0$ deg $(\phi_{fe} - 2\phi_{se})$
ϕ_f = local phase of the fundamental wave
ϕ_{fe} = initial phase of the helical fundamental wave [Eq. (1)]
ϕ_h = local phase of the first-harmonic wave
ϕ_s = local phase of the subharmonic wave
ϕ_{se} = initial phase of the axisymmetric subharmonic wave [Eq. (3)]

Subscripts

c = jet center
e = jet exit
f = fundamental
h = harmonic
m = maximum value
s = subharmonic

Superscript

$'$ = rms

I. Introduction

BECAUSE the entrainment ability and mixing potential of jets are of great interest in a variety of engineering applications, many efforts have been made to understand and control jet flows. An initial disturbance has significant effects on the development of large-scale vortical structures in the near field of an axisymmetric jet.[1–3] In anticipation of mixing enhancement, vortex pairing control, and jet noise reduction, many studies have been carried out with axisymmetric disturbances,[4–9] where the mean flow remains axisymmetric. Recently, attention has been given to three-dimensional disturbances, in particular, helical mode forcing.[10–18] Under a single helical mode forcing,[13] the periodic time series of sound pressure from each individual speaker located at an azimuthal angle γ would be $p = p_m \sin(2\pi f t + m\gamma)$. In addition, by forcing with two superposed helical waves of the same frequency, spinning in the opposite directions, the shape of the jet cross section can be significantly changed. In this case the helical waves exhibit azimuthal variations of amplitude and grow downstream from intermodal resonant interactions. In fact, two-lobed and four-lobed jet cross sections were generated by forcing the jet with helical mode pairs with the same frequency and equal but opposite azimuthal wave numbers, $m = \pm 1$ and ± 2[17], respectively. Cohen and Wygnanski[12] showed theoretically and experimentally that changes in the shape of the jet cross section are because of resonant interaction between the two helical waves.

Under axisymmetric forcings, on the other hand, vortex pairing occurs axisymmetrically and plays a key role in mixing enhancement. The growth of the initial subharmonic wave via subharmonic resonance leads to a downstream pairing of neighboring vortices.[5] Furthermore, vortex pairing (that is, subharmonic growth) is sensitive to the initial phase difference between the fundamental and its subharmonic and to some extent can be precisely controlled by varying the initial phase difference.[7–9]

Therefore, the combined forcing, which consists of the helical fundamental waves and the axisymmetric subharmonic wave with initially controlled phase difference between them, can enhance vortex pairing, which is different from that observed for axisymmetric forcing, and thus significantly changes the shape of the jet cross

Presented as Paper 98-0783 at the AIAA 36th Aerospace Sciences Meeting, Reno, NV, 12–15 January 1998; received 11 May 1998; revision received 13 July 1999; accepted for publication 12 August 1999.

*Ph.D. Student, School of Mechanical and Aerospace Engineering; currently Postdoctoral Research Fellow, Mechanical and Aerospace Engineering Department, University of California, Los Angeles, Los Angeles, CA 90095; skc@ucla.edu. Member AIAA.

†Professor, School of Mechanical and Aerospace Engineering; jyyoo@plaza.snu.ac.kr. Member AIAA.

‡Assistant Professor, School of Mechanical and Aerospace Engineering; choi@socrates.snu.ac.kr. Member AIAA.

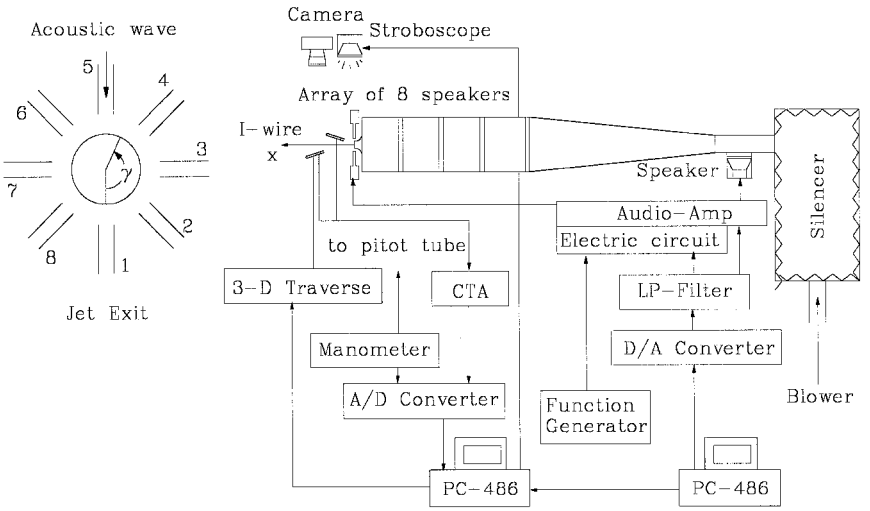

Fig. 1 Schematic layout of the experimental apparatus.

section. Corke and Kusek[18] showed that the helical modes were rapidly amplified downstream through resonant interaction, when the helical fundamental mode pair ($m_f = \pm 1$) together with an axisymmetric harmonic mode ($m_h = 0$) was introduced near the jet exit. Eventually, vortex pairing of helical modes occurred in the downstream region, and the momentum thickness of the shear layer varied in the azimuthal direction. In the present study an axisymmetric jet is acoustically forced with helical fundamental waves of an identical frequency spinning in the opposite directions ($m_f = \pm 1$) and an axisymmetric subharmonic wave ($m_s = 0$). In addition, the initial phase difference between the helical fundamentals and the axisymmetric subharmonic is carefully controlled. The objectives are to study the subharmonic resonance between the helical fundamental waves and the axisymmetric subharmonic wave and to investigate the effect of the initial phase difference between them on the growth of the subharmonic (vortex pairing of helical modes) and the evolution of the jet cross section.

II. Experimental Technique

The experimental apparatus consisted of an air-jet facility, an acoustic forcing system, a data acquisition system, and a flow visualization system, as shown in Fig. 1.

A. Air-Jet Facility

Airflow from a blower passed through a silencer box, a diffuser, and a settling chamber equipped with three screens and a honeycomb straightener before exiting through an American Society of Mechanical Engineers flow nozzle. The nozzle with a contraction ratio of 76:1 and an exit diameter of $D = 32.1$ mm was selected to achieve very thin boundary-layer thickness at the exit. At the exit velocity $U_e = 8.6$ m/s, the nonuniformity of the flow at the jet exit was less than 0.8%, and the turbulence level was 0.3%. A large portion of the turbulence level was at very low frequencies of less than 20 Hz. The exit velocity measured at $x = 0.1$ mm exhibited a top-hat velocity profile, surrounded by a thin shear layer with a shape factor of 2.6, which agrees well with that of the Blasius profile.[9] The maximum value of turbulence level in this shear layer was 0.5%.

B. Acoustic Forcing System

Two sinusoidal signals, one for the $m_f = \pm 1$ helical fundamental modes and the other for the axisymmetric subharmonic mode, were generated by a D/A converter (DT 2838) connected to an IBM PC486. Between them there was one octave difference in frequency and a variable phase difference. The fundamental sine wave was transmitted to an electric circuit and an audio amplifier where eight independent signals for the $m_f = \pm 1$ helical modes were generated and amplified. Then, they were transmitted to an array of eight speakers and waveguides, which were located close to the nozzle lip and equally spaced in azimuthal angle (for more details, see Ref. 19). This array of eight speakers and waveguides was designed to be rotatable around the jet centerline so that it was possible to make velocity measurements and to take photographs of the visualized jet sections on various meridional planes without actually rotating the measuring probe and the flow visualization system. The sound pressures from eight speakers were independently controlled in the electric circuit in terms of both amplitude and phase according to the following equations:

$$p/p_m = \sin(2\pi f t + \gamma - \phi_{\mathrm{fe}}) + \sin(2\pi f t - \gamma - \phi_{\mathrm{fe}}) \quad (1)$$

$$= 2\cos\gamma \sin(2\pi f t - \phi_{\mathrm{fe}}) \quad (2)$$

The first and second terms on the right-hand side of Eq. (1) represent the $m_f = +1$ mode and the $m_f = -1$ mode helical waves, respectively. A microphone (Larson·Davis 2560) mounted on the jet centerline at the exit plane was used to check the sound level of each speaker for the no-flow condition. The maximum sound level p_m was set at 84.6 dB, at which the amplitude of the helical modes was high enough so that nonlinear interaction between the waves occurred immediately downstream of the jet exit.

The axisymmetric subharmonic forcing ($m_s = 0$) was accomplished by a 4-in.-diam speaker mounted on the pipe wall preceding the diffuser. The initial axisymmetric subharmonic wave was introduced in the form of velocity fluctuation at the jet exit as follows:

$$u/U_e = \sqrt{2} a_s \sin(\pi f t - \phi_{\mathrm{se}}) \quad (3)$$

where the initial subharmonic amplitude a_s was defined by the rms value of the u signal measured at the jet exit. In the present experiment it was 0.7%. The local phase difference between the fundamental and subharmonic modes was defined as

$$\phi_d = \phi_f - 2\phi_s \quad (4)$$

which was obtained by the autobispectrum[20] through a fast Fourier transform calculation of the u signal. The initial phase difference $\phi_{\mathrm{de}} = \phi_{\mathrm{fe}} - 2\phi_{\mathrm{se}}$ was also calculated in the same way from the u signal measured at $x/D = 0$, $r/D = 0.25$, and $\gamma = 0$ deg.

C. Data Acquisition System

To simultaneously obtain velocity data at two positions, two I-type hot-wire probes (Dantec 55P11), a reference probe, and a measuring probe were used in conjunction with the constant-temperature hot-wire anemometer (Dantec Streamline). The output signals of the hot wire were converted through a 16-bit A/D converter (DT 2838), stored, and afterward reduced to velocity data with a fourth-order polynomial. Uncertainty estimates of hot-wire data were made based on Yavuzkurt,[21] considering the following factors: a calibration uncertainty of the hot wire (0.8%), a room temperature drift during experiments (0.3°C), and an uncertainty in flow condition setting (1%). The uncertainties for both the streamwise mean velocity U and the streamwise velocity fluctuation u were 1.6% along

the centerline. In the shear layer they were estimated to be greater than 3.3%, considering higher velocity fluctuations and flow reversal. The reference probe was fixed at $x/D = 1.5$, $r/D = 0.25$, and $\gamma = 180$ deg. The movement of the measuring probe was controlled two-dimensionally by the PC. Measurements were made at eight azimuthal positions equally spaced by an angle of 45 deg.

D. Flow Visualization System

A multi-smoke-wire technique was employed to visualize the time sequence of the jet structure downstream of the jet exit. A number of thin nichrome wires (80 μm in diameter) were placed perpendicularly to the jet axis at an interval of $0.5D$ up to $x/D = 3$ and at an interval of $1D$ thereafter. A stroboscope was synchronized with the fundamental or subharmonic signal from the D/A converter. All of the photos were taken at two phases of the fundamental wave or three phases of the subharmonic wave with the camera lens open.

III. Results and Discussion

A. Forcing with only a Helical Mode Pair ($m = \pm 1$)

First, let us consider the vortex structures for three helical-mode-forcing conditions, two of which are schematically shown in Fig. 2. Here, Fig. 2 is drawn based on previous flow visualization images.[13,15,16] For $m = +1$ mode forcing, of which sound pressure disturbance at the jet exit corresponds to the first term on the right-hand side of Eq. (1), a continuous vortex rolls up, which resembles a coil spring spinning in the counterclockwise direction when it is viewed in the upstream direction (Fig. 2a). For $m = -1$ mode forcing the sound pressure disturbance corresponds to the second term on the right-hand side of Eq. (1), and the vortex structure is the same as that of $m = +1$ mode forcing but with the opposite spinning direction. Koch et al.[13] showed this single continuous vortex structure using flow visualization. In both cases the distortion of the jet cross section does not appear, but the jet spreads out axisymmetrically because the resultant forcings are imposed equally over the entire jet circumference.[12]

On the other hand, when the jet is forced with a helical mode pair having the same frequency and equal but opposite azimuthal wave numbers $m = \pm 1$, as described in Eq. (2), there exists an azimuthal variation of the helical-mode input amplitude [see Eq. (2)]. The superposition of the two helical waves physically produces a standing wave pattern. As schematically shown in Fig. 2b, strong vortices alternately roll up at the azimuthal locations of $\gamma = 0$ and 180 deg (180 deg out of phase), whereas weak vortices roll up at $\gamma = 90$ and 270 deg (in phase).

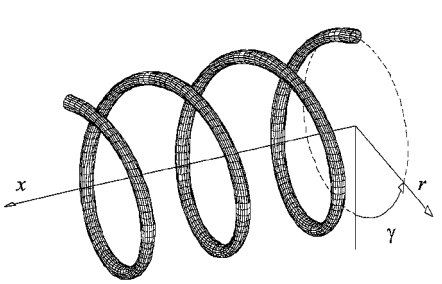

a) $m = +1$

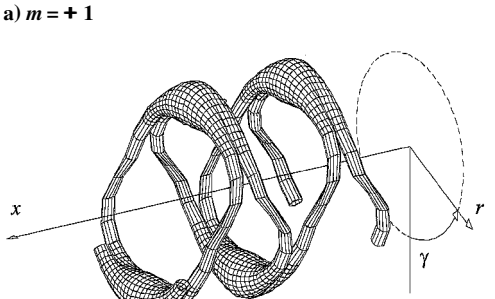

b) $m = \pm 1$

Fig. 2 Sketches of the vortex structures for various helical mode forcing conditions. Dashed circle denotes the jet exit.

Figure 3 shows multi-smoke-wire flow visualization of the vortex structure when the jet is forced with an $m = \pm 1$ helical mode pair at $U_e = 8.6$ m/s and $f = 160$ Hz ($Sr_D = 0.6$). The vortex structure observed is similar to that schematically shown in Fig. 2b. Figure 3a shows that at time t strong vortices are rolling up roughly in a staggered formation along the flow direction on the (r, x) planes at $\gamma = 0$ and 180 deg (hereafter called the $\gamma = 0$–180 deg plane; see also Fig. 2b). However, vortices at $x/D = 1.0$–1.5 and at time $t + \Delta t$ in Fig. 3a look in-phase as if they were triggered by an axisymmetric forcing, which is caused by the growth of the harmonic wave from intermodal interaction between the fundamentals, indicating that vortices roll up twice as much as those rolled up at the fundamental frequency. This growth of the harmonic wave was also shown in the hot-wire measurements of Long and Petersen.[17] Figure 3b shows the vortex structure on the $\gamma = 45$–225 deg plane, where staggered strong vortices are clearly observed. On the $\gamma = 90$–270 deg plane (Fig. 3c), however, weak vortices at $x/D = 1 \sim 2$ are in phase and placed in the middle of the strong staggered vortices that exist on the $\gamma = 0$–180 and 45–225 deg planes. Moreover, the vortex on the $\gamma = 90$–270 deg plane rolls up twice as much as the strong staggered vortex, also resulting from the growth of the harmonic wave. The weak vortices connect the strong staggered vortices and produce a characteristic Y pattern when looking perpendicular to the $\gamma = 0$–180 deg plane (see Fig. 2b). This Y pattern was also observed experimentally by Kusek et al.[15] and numerically by Martin.[16]

Under forcing with the $m = \pm 1$ helical mode pair at $Sr_D = 0.6$, a two-lobed shape of the jet cross section was observed (not shown in this paper; refer to Cho[19] and Long and Petersen[17]). The high and low amplitude levels of the helical fundamental waves (strong and weak vortices, respectively) corresponded to major and minor axes of the two-lobed shape of the jet cross section, respectively. Vortex pairing did not occur in this case ($Sr_D = 0.6$), as shown in Fig. 3.

B. Subharmonic Modulation under $m = \pm 1$ Helical Mode Forcing at a Higher Sr_D

When the jet is forced with the same $m = \pm 1$ helical fundamental mode pair but at a higher Sr_D, a vortex can easily interact with the preceding vortex, and vortex pairing occurs intermittently. Although the subharmonic is not added initially, its growth may be initiated by the subharmonic disturbance of an extremely low amplitude level originated from the test facility itself or pairing feedback. In the event that this naturally initiated subharmonic grows high, the jet cross section is not the two-lobed shape but changes into a rectangular shape, as shown in Fig. 4, depending on which azimuthal position vortex pairing occurs more frequently. In fact, in the case of forcing with only $m = \pm 1$ helical fundamental mode pair at $Sr_D = 0.95$, we can observe frequency halvings of the u signal (Fig. 5). The subharmonic component grows from an imperfect resonant interaction, which is also triggered by facility disturbances or pairing feedback. Moreover, we note that there exist modulations in amplitude, as shown in Fig. 5. These modulations, which are denoted as nearly periodic modulations of pairing in Broze and Hussain's experiment,[22] are caused by the inability of the subharmonic to phase-lock. In other words, the initial phase difference between the fundamental and the subharmonic initiated by facility disturbances or pairing feedback does not remain the same from one pairing to the next.

C. Forcing with Helical Fundamental Mode Pair and Additional Axisymmetric Subharmonic Mode

Subharmonic Resonance

An axisymmetric subharmonic mode ($m_s = 0$) is introduced in addition to a helical fundamental mode pair ($m_f = \pm 1$) at $Sr_D = 0.78$. In this case the frequencies of the helical fundamental and the axisymmetric subharmonic are 250 and 125 Hz, respectively, and U_e is 10.3 m/s ($Re_D = 2.2 \times 10^4$). Measurements are made at an upstream location of vortex pairing ($x/D = 1.5$) and at two azimuthal locations of the high-speed side of the shear layer ($\gamma = 0$ and 180 deg at $r/D = 0.25$). Note that the initial phase difference ϕ_{de} is defined to be the local phase difference between the fundamental and the subharmonic at $\gamma = 0$ deg on the jet-exit plane. The local phase difference between the fundamental and the subharmonic at $\gamma = 180$ deg is different by 180 deg from that at $\gamma = 0$ deg (or ϕ_{de}), that is,

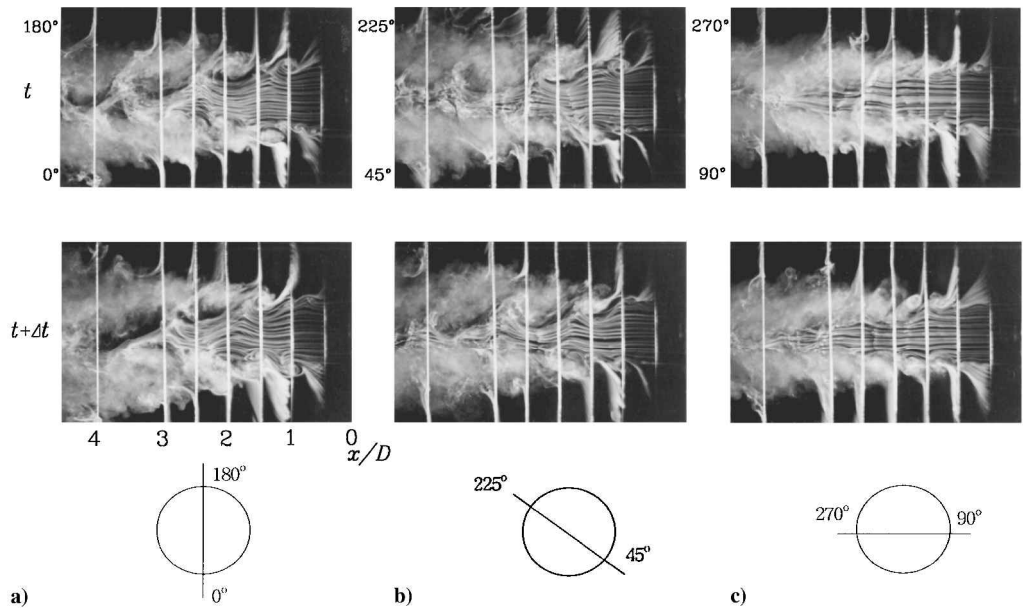

Fig. 3 Flow visualization of the structure of the jet forced with only the $m = \pm 1$ helical mode pair at $Sr_D = 0.6$ on the a) $\gamma = 0$–180 deg plane, b) $\gamma = 45$–225 deg plane, and c) $\gamma = 90$–270 deg plane. The time interval of $\Delta t = 3.125$ ms corresponds to one-half of the forcing wave period.

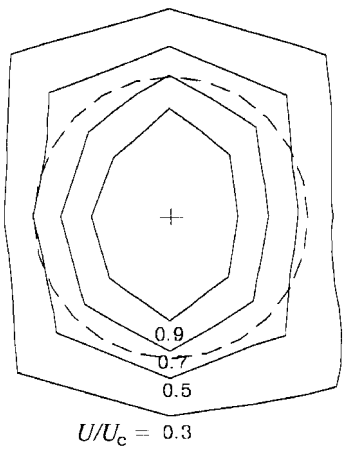

Fig. 4 Iso-velocity contour lines (U/U_c) for forcing with only the $m = \pm 1$ helical mode pair at $Sr_D = 0.78$ and $x/D = 3$. Dashed circle denotes the jet exit.

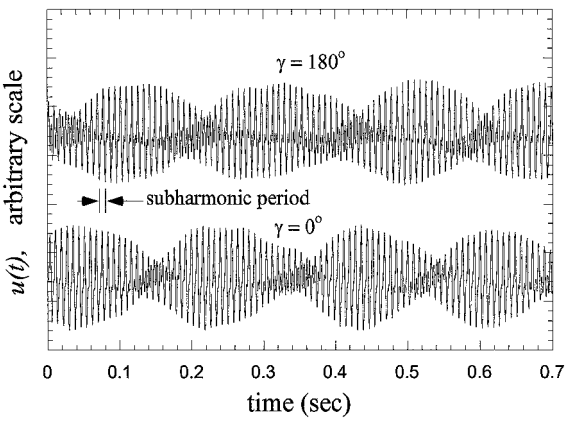

Fig. 5 Time traces of the u signal at $x/D = 1.5$, $r/D = 0.25$, and $Sr_D = 0.95$ for forcing with only the $m = \pm 1$ helical mode pair.

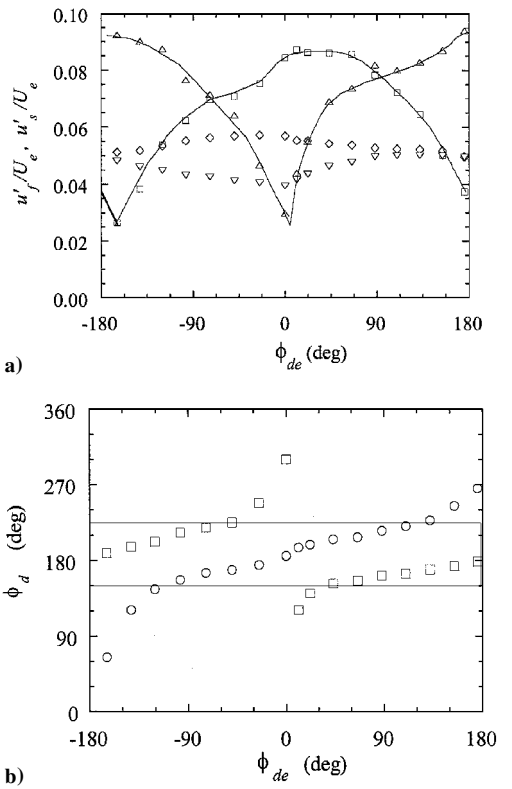

Fig. 6 Variations of the wave amplitude (u'_f and u'_s) and the local phase difference ϕ_d with respect to the initial phase difference ϕ_{de} for the case of forcing with a helical fundamental mode pair ($m_f = \pm 1$) and an additional axisymmetric subharmonic mode ($m_s = 0$) at $Sr_D = 0.78$: a) □, u'_s at $\gamma = 180$ deg; ◇, u'_f at $\gamma = 180$ deg; △, u'_s at $\gamma = 0$ deg; ▽, u'_f at $\gamma = 0$ deg; b) ○, $\phi_d|_{\gamma = 180\ \mathrm{deg}}$; □, $\phi_d|_{\gamma = 0\ \mathrm{deg}}$. Measurements were made at $x/D = 1.5$ and $r/D = 0.25$.

$\phi_d|_{\gamma = 180\,\mathrm{deg}} - \phi_d|_{\gamma = 0\,\mathrm{deg}} = 180$ deg according to Eq. (4), which is caused by the fact that the fundamental waves at $\gamma = 0$ and 180 deg are 180 deg out of phase, while the subharmonic waves at $\gamma = 0$ and 180 deg are in-phase because the initial subharmonic wave is axisymmetric (corresponding to a bulk modulation of the jet-exit velocity over the entire jet-exit plane). Considering that the phase difference may significantly affect vortex interaction, this is quite noteworthy in the sense that an asymmetric flowfield can be generated between the upper (90 deg $< \gamma <$ 270 deg) and lower (−90 deg $< \gamma <$ 90 deg) sides of the jet cross section.

Variations of the wave amplitude with the initial phase difference ϕ_{de} are shown in Fig. 6a. Note that ϕ_{de} has a significant effect on the growth of the subharmonic component u'_s. Although the initial amplitude of the subharmonic component a_s is very low (0.7%) at the jet exit, u'_s at $x/D = 1.5$ is rapidly amplified over the fundamental amplitude u'_f except at some critical values of ϕ_{de} (close to 10 deg at

$\gamma = 0$ deg and close to -170 deg at $\gamma = 180$ deg). Variations of the subharmonic amplitude u'_s at both $\gamma = 0$ and 180 deg show cusplike shapes. A similar cusplike variation of the subharmonic component was also observed under axisymmetric forcings in Refs. 8 and 9. Based on the assumption of a parallel nondiverging flow, Monkewitz[23] predicted that the subharmonic is suppressed at a critical value of the phase difference and amplified over a wide range of the phase difference. Also note from Fig. 6a that, when the variation curve of the subharmonic obtained with the initial phase difference at $\gamma = 180$ deg is moved to the right by 180 deg, the two curves approximately fall on each other. This is because of the discrepancy of 180 deg in the local phase differences between the fundamental and the subharmonic at $\gamma = 0$ and 180 deg on the jet-exit plane, as mentioned earlier.

Under the present forcing condition, an asymmetric flowfield between the upper (90 deg $< \gamma <$ 270 deg) and lower (-90 deg $< \gamma <$ 90 deg) sides of the jet cross section can be generated by varying ϕ_{de}. At $\phi_{de} \approx 10$ deg, $u'_s|_{\gamma = 180\,\text{deg}}$ is maximum while $u'_s|_{\gamma = 0\,\text{deg}}$ is minimum, and vice versa at $\phi_{de} \approx -170$ deg. This is quite noteworthy because ϕ_{de} can be used as one of the important parameters in changing and controlling the shape of the jet cross section under the present forcing condition. Such an asymmetric flow does not occur under forcing of the helical fundamental mode pair combined with the axisymmetric first-harmonic mode (i.e., $2f$ with $m_h = 0$) (Ref. 18), as well as under forcing with only a helical mode pair.[17] In the former case the local phase difference between the fundamental and the first harmonic ($\phi_h - 2\phi_f$) is the same over the entire jet cross section, and thus the flowfield is symmetric with respect to the $\gamma = 90$–270 deg plane.

Variations of the local phase difference between the fundamental and its subharmonic with the initial phase difference are shown in Fig. 6b, which are obtained from the autobispectrum of u signal. The local phase differences do not deviate too far from 180 deg regardless of ϕ_{de}, except for $\phi_{de} \approx -170$ deg at $\gamma = 180$ deg and for $\phi_{de} \approx 10$ deg at $\gamma = 0$ deg. This indicates that the fundamental and the subharmonic are phase-locked, and resonant interaction between them occurs as shown by Broze and Hussain.[24] This phase-locking is a prerequisite to subharmonic resonance from which the subharmonic component rapidly grows, eventually resulting in vortex pairing.

The time traces of the u signal at three different initial phase differences are shown in Fig. 7. Frequency halvings of the u signal occur, significantly depending on ϕ_{de}. At $\phi_{de} = 10$ deg (maximum subharmonic growth at $\gamma = 180$ deg and minimum subharmonic growth at $\gamma = 0$ deg), frequency halving is enhanced at $\gamma = 180$ deg and attenuated at $\gamma = 0$ deg (Fig. 7a). At $\phi_{de} = -170$ deg, the opposite is observed, as shown in Fig. 7b. At $\phi_{de} = -76$ deg, where levels of the subharmonic at $\gamma = 0$ and 180 deg are nearly equal to each other, the frequency halvings at both azimuthal positions are comparable to each other, as shown in Fig. 7c (see also Fig. 6a).

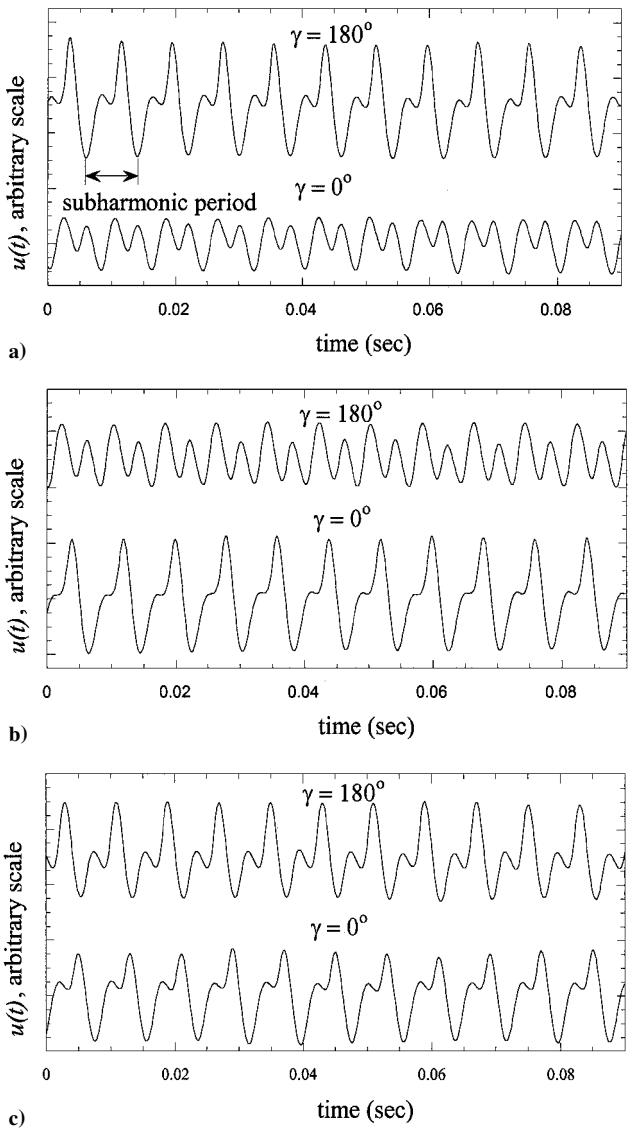

Fig. 7 Time traces of the u signal at three different initial phase differences at $Sr_D = 0.78$, $x/D = 1.5$, and $r/D = 0.25$: a) $\phi_{de} = 10$ deg; b) $\phi_{de} = -170$ deg; and c) $\phi_{de} = -76$ deg.

Flow Visualization

The multi-smoke-wire flow visualization has been also performed for the same forcing condition at $Sr_D = 0.78$ and $\phi_{de} = 10$ deg, where the subharmonic wave at $\gamma = 180$ deg is amplified and that at $\gamma = 0$ deg is attenuated (refer to Fig. 6a). Figure 8 shows the vortex structures on three (r, x) planes, that is, $\gamma = 0$–180 deg, $\gamma = 45$–225 deg, and $\gamma = 90$–270 deg planes. The time interval of $\Delta t = 2.7$ ms corresponds to one-third of the subharmonic period. All photographs show that up to $x/D = 1$ a typical vortex structure under forcing with only $m = \pm 1$ helical mode pair appears (see also Fig. 3): strong vortices on the $\gamma = 0$–180 deg plane and on the $\gamma = 45$–225 deg plane are staggered, whereas weak vortices on the $\gamma = 90$–270 deg plane are in phase. Thereafter, a large vortex begins to interact with its preceding vortex, which can either pair or not. We can clearly observe from Fig. 8a that vortices at $\gamma = 180$ deg are completely pairing near $x/D = 2$, while five vortices at $\gamma = 0$ deg are advecting downstream without pairing before they finally break down. This flow visualization evidently explains the different growth rates of the subharmonic component, observed in Fig. 6a, at $\gamma = 0$ and 180 deg with $\phi_{de} = 10$ deg. On the other hand, at $\gamma = 45$ deg (Fig. 8b), vortex pairing occurs farther downstream (at $x/D = 2 \sim 3$), occupying a wide space. In fact, vortex pairing has a significant effect on the jet mixing and leads to a large mixing rate. Note from Fig. 8a that the spreading rate at $\gamma = 180$ deg is larger than that at $\gamma = 0$ deg. On the $\gamma = 90$–270 deg plane (Fig. 8c) weak vortices that connect the strong vortices also pair and form into a large vortex. However, the jet-spreading rate is not so large as compared to those on other planes. A quantitative description about the jet spreading is given later in this section.

Browand and Laufer[10] first reported a pairing motion of a single helical vortex. This motion was later numerically simulated by Martin,[16] who enforced a single fundamental helical mode plus an axisymmetric mode of $\frac{2}{3}f$ on the axisymmetric jet and denoted the resulting motion as helical pairing. In the meantime, with an additional first-harmonic axisymmetric mode to the $m = \pm 1$ helical mode pair, Kusek et al.[14] and Corke and Kusek[18] showed a similar vortex pairing motion to the one observed in this study, which was denoted as vortex pairing of helical modes. Especially in Ref. 18, the vortex structure generated after vortex pairing was tilted along the streamwise direction, and its resultant mode was exactly $m = \pm 1$ helical (that is, amplitudes of the subharmonic are maxima at $\gamma = 0$ and 180 deg, and minima at $\gamma = 90$ and 270 deg). In the present study the vortex structure is also tilted, as shown in Figs. 8a and 8b. However, the resultant wave mode is far from the $m = \pm 1$ helical mode pair in terms of the variation of the subharmonic growth with respect to the azimuthal position and the shape of the jet cross section, which results from the asymmetry of the initial local phase

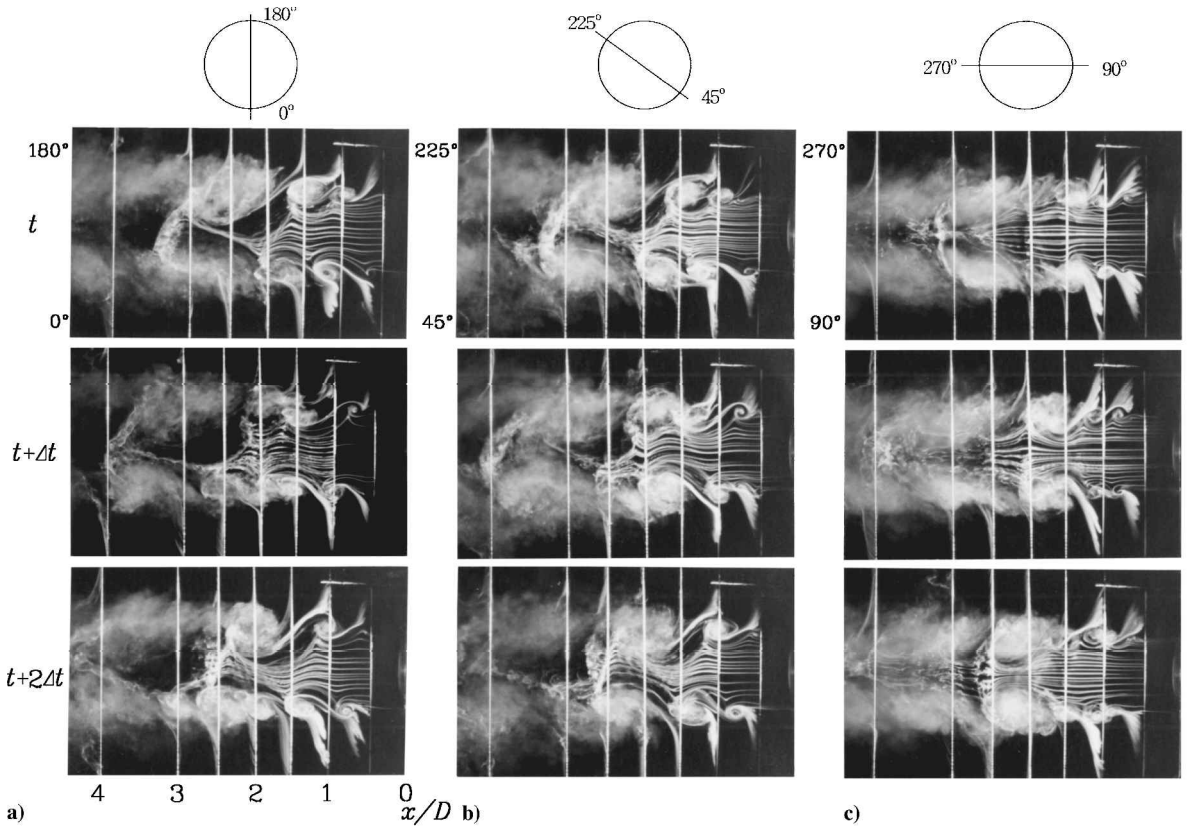

Fig. 8 Flow visualization of the structure of the jet forced with the helical fundamental mode pair and the axisymmetric subharmonic mode at $Sr_D = 0.78$ and $\phi_{de} = 10$ deg on the a) $\gamma = 0$–180 deg plane, b) $\gamma = 45$–225 deg plane, and c) $\gamma = 90$–270 deg plane. The time interval of $\Delta t = 2.7$ ms corresponds to one-third of the subharmonic period.

difference with respect to the $\gamma = 90$–270 deg plane as well as the different forcing amplitude and Sr_D.

Jet Cross Section

Vortex pairing results in a change in the shape of the jet cross section. Iso-velocity contours on the jet cross section at four different streamwise positions are given in Fig. 9. The initial subharmonic was added at $\phi_{de} = -170$ deg, which corresponds to an enhanced subharmonic growth at $\gamma = 0$ deg and an attenuated subharmonic growth at $\gamma = 180$ deg (refer to Fig. 6a). The vortex structure for this case is nearly the same as that shown in Fig. 8 when the coordinate system is rotated by 180 deg around the jet centerline. At $x/D = 1.5$ where vortex pairing just starts, no significant change is observed in the shape of the jet cross section, but the lower side (-90 deg $< \gamma <$ 90 deg) spreads out a little more than the upper side (90 deg $< \gamma <$ 270 deg). However, the shape of the jet cross section at $x/D > 2$ significantly changes. The shape of the jet cross section is neither two lobed nor four lobed but three lobed. At $\gamma = 0$, 135, and 225 deg, vortex pairing occurs, and the jet widely spreads out away from the jet centerline, generating three lobes in the jet cross section. To the best of the authors' knowledge, this three-lobed jet cross section has never been reported in the literature before. The momentum thicknesses at $\gamma = 0$, 135, and 225 deg, representing the mixing rate, are much larger than those at other γ or that of the unforced jet, as shown in Fig. 10. Evolution of the radial position $r_{0.1}$ in x also shows nearly the same behavior (not included in this paper) as shown in Fig. 10. Figure 11 shows the rms streamwise velocity fluctuation u' and its subharmonic component u'_s at $x/D = 3$. Both u' and u'_s are large at the locations of three lobes, and u'_s contributes to most of u' at those locations.

The response of the jet cross section at $x/D = 3$ to the initial phase difference can be roughly estimated in terms of the differences among the mean velocities at three azimuthal positions. The difference between the mean velocities at $\gamma = 0$ and 180 deg is shown in Fig. 12a, and the difference between those at $\gamma = 225$ and 180 deg

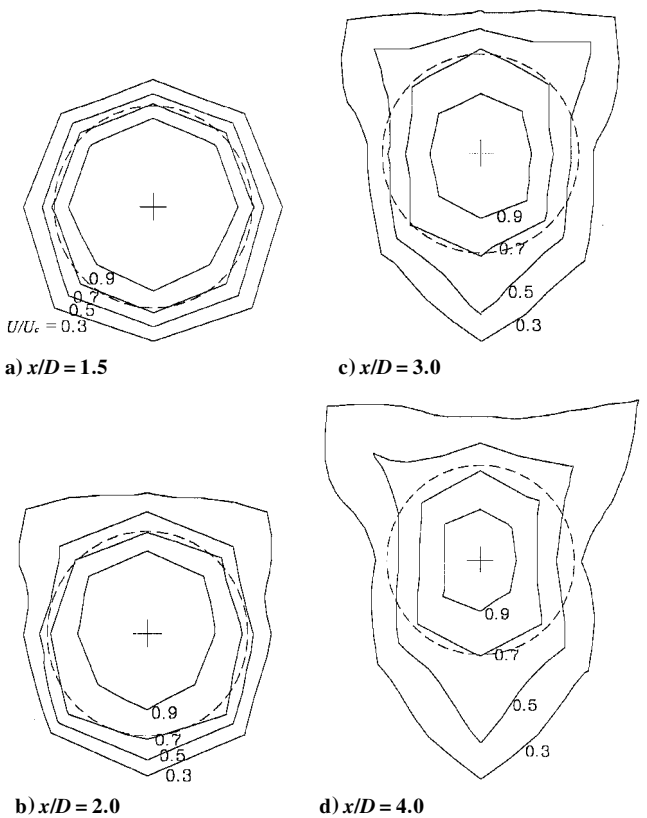

Fig. 9 Iso-velocity contour lines (U/U_c) on the jet cross section under forcing with the helical fundamental mode pair and the axisymmetric subharmonic mode at $Sr_D = 0.78$ and $\phi_{de} = -170$ deg. Dashed circles denote the jet exit.

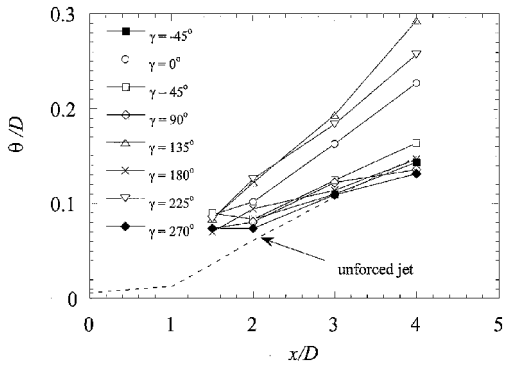

Fig. 10 Streamwise evolution of the momentum thickness at various azimuthal locations under forcing with the helical fundamental mode pair and the axisymmetric subharmonic mode, compared with that of the unforced jet ($Re_D = 1.9 \times 10^4$).

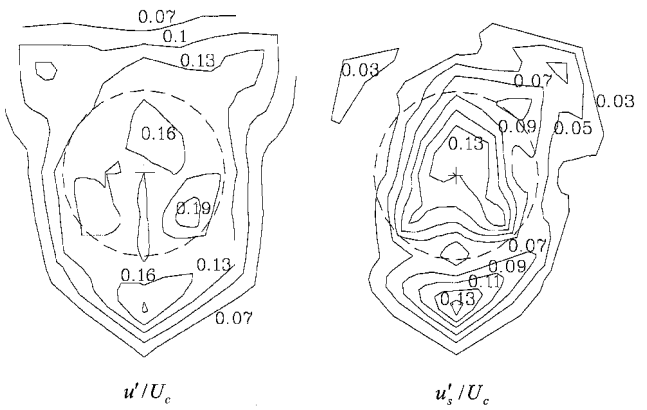

Fig. 11 Contours of the rms streamwise velocity fluctuation u' and its subharmonic component u'_s at $x/D = 3$, $Sr_D = 0.78$, and $\phi_{de} = -170$ deg under forcing with the helical fundamental mode pair and the axisymmetric subharmonic mode. Dashed circles denote the jet exit.

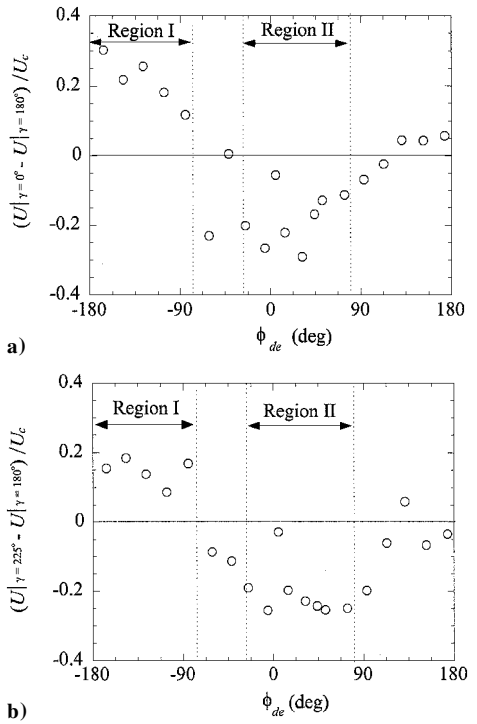

Fig. 12 Mean velocity differences between two azimuthal positions at $x/D = 3$ and $r/D = 0.75$ with respect to ϕ_{de} for the case of forcing with the helical fundamental mode pair and the axisymmetric subharmonic mode at $Sr_D = 0.78$. Region I corresponds to the three-lobed-cross-section case; region II, to the similar shape rotated 180 deg.

is shown in Fig. 12b. The data away from zero mean-velocity difference in Fig. 12 indicate that the jet cross section has lobes and its shape deviates from a circle. Based on the mean-velocity difference, region I (where the shape of the jet cross section is three lobed and similar to that in Fig. 9c) and region II (where the shape of the jet cross section is the same as in Fig. 9c but rotated by 180 deg around the jet centerline) can be identified. These two regions include two critical initial phase differences, $\phi_{de} = -170$ and 10 deg, at which the subharmonic levels at $\gamma = 0$ and 180 deg have maximum or minimum values, as shown in Fig. 6a. The jet cross sections in the remaining region of ϕ_{de} correspond to intermediate states between regions I and II, where the three-lobed jet cross section does not appear distinctly. The present result clearly shows that the initial phase difference can change and control the shape of the jet cross section through vortex pairing control.

IV. Conclusions

An experimental study has been performed to consider the effect of the forcing conditions on the vortex structure of an axisymmetric jet, which includes multi-smoke-wire flow visualizations and hot-wire measurements.

First, the axisymmetric jet is forced only with a helical mode pair ($m = \pm 1$) near the jet exit ($Sr_D = 0.6$). On the $\gamma = 0$–180 and 45–225 deg planes, strong staggered vortices roll up, whereas weak vortices on the $\gamma = 90$–270 deg plane connect these strong vortices. The shape of the jet cross section changes downstream and becomes two-lobed. At a higher Sr_D ($Sr_D = 0.78$) the shape becomes rectangular in the case that the naturally initiated subharmonic grows high. At $Sr_D = 0.95$ the subharmonic component grows from imperfect resonant interaction, and there exist modulations of the u signal in amplitude.

Next, the axisymmetric jet is forced with a helical fundamental mode pair ($m_f = \pm 1$) and an additional axisymmetric subharmonic mode ($m_s = 0$) near the jet exit ($Sr_D = 0.78$). The subharmonic component rapidly grows downstream from resonant interaction (subharmonic resonance) with the fundamental, significantly depending on the initial phase difference between the fundamental and subharmonic waves. The variation of the subharmonic amplitude with the initial phase difference shows a cusplike shape. The amplification of the subharmonic results in vortex pairing of helical modes. Because the local phase difference between the fundamental and its subharmonic on the upper side of the jet cross section at the jet exit is 180 deg different from that on the lower side, an asymmetric flowfield is generated depending on which azimuthal position vortex pairing occurs. Near critical initial phase differences where the subharmonic at $\gamma = 0$ deg has a maximum value and that at $\gamma = 180$ deg has a minimum value, or vice versa, the jet has a three-lobed cross section. The lobes are generated by vortex pairing. The appearance of the three-lobed jet cross section significantly depends on the initial phase difference. As a result, the initial phase difference between the fundamental helical mode pair and the axisymmetric subharmonic mode is an important parameter in changing and controlling the shape of the jet cross section.

Acknowledgments

The authors wish to express their deepest gratitude for the financial support of the Ministry of Education and of the Turbo and Power Machinery Research Center throughout this work. H. Choi acknowledges the support from the Korean Ministry of Science and Technology through the Creative Research Initiatives.

References

[1] Ho, C.-M., and Huerre, P., "Perturbed Free Shear Layers," *Annual Review of Fluid Mechanics*, Vol. 16, 1984, pp. 365–424.

[2] Thomas, F. O., "Structure of Mixing Layers and Jets," *Applied Mechanics Reviews*, Vol. 44, No. 3, 1991, pp. 119–153.

[3] Mankbadi, R. R., "Dynamics and Control of Coherent Structure in Turbulent Jets," *Applied Mechanics Reviews*, Vol. 45, No. 6, 1992, pp. 219–247.

[4] Crow, S. C., and Champagne, F. H., "Orderly Structure in Jet Turbulence," *Journal of Fluid Mechanics*, Vol. 48, Pt. 3, 1971, pp. 547–591.

[5] Zaman, K. B. M. Q., and Hussain, A. K. M. F., "Vortex Pairing in a Circular Jet Under Controlled Excitation. Part 1. General Jet Response," *Journal of Fluid Mechanics*, Vol. 101, Pt. 3, 1980, pp. 449–491.

[6]Arbey, H., and Ffowcs Williams, J. E., "Active Cancellation of Pure Tones in an Excited Jet," *Journal of Fluid Mechanics*, Vol. 149, 1984, pp. 445–454.

[7]Paschereit, C. O., Wygnanski, I., and Fiedler, H. E., "Experimental Investigation of Subharmonic Resonance in an Axisymmetric Jet," *Journal of Fluid Mechanics*, Vol. 283, 1995, pp. 365–407.

[8]Husain, H. S., and Hussain, F., "Experiments on Subharmonic Resonance in a Shear Layer," *Journal of Fluid Mechanics*, Vol. 304, 1995, pp. 343–372.

[9]Cho, S. K., Yoo, J. Y., and Choi, H., "Vortex Pairing in an Axisymmetric Jet Using Two-Frequency Acoustic Forcing at Low to Moderate Strouhal Numbers," *Experiments in Fluids*, Vol. 25, No. 4, 1998, pp. 305–315.

[10]Browand, F. K., and Laufer, J., "The Role of Large Scale Structures in the Initial Development of Circular Jets," *Proceedings of 4th Biennial Symposium on Turbulence in Liquids*, edited by J. L. Zakin and G. K. Patterson, Science Press, Princeton, NJ, 1975, pp. 333–344.

[11]Strange, P. J. R., and Crighton, D. G., "Spinning Modes on Axisymmetric Jets. Part 1," *Journal of Fluid Mechanics*, Vol. 134, 1983, pp. 231–245.

[12]Cohen, J., and Wygnanski, I., "The Evolution of Instabilities in the Axisymmetric Jet. Part 2. The Flow Resulting from the Interaction Between Two Waves," *Journal of Fluid Mechanics*, Vol. 176, 1987, pp. 221–235.

[13]Koch, C. R., Mungal, M. G., Reynolds, W. C., and Powell, J. D., "Helical Modes in an Acoustically Excited Round Air Jet," *Physics of Fluid A*, Vol. 1, No. 9, 1989, p. 1443.

[14]Kusek, S. M., Corke, T. C., and Reisenthel, P., "Control of Two and Three Dimensional Modes in the Initial Region in an Axisymmetric Jet," AIAA Paper 89-0968, March 1989.

[15]Kusek, S. M., Corke, T. C., and Reisenthel, P., "Seeding of Helical Modes in the Initial Region of an Axisymmetric Jet," *Experiments in Fluids*, Vol. 10, No. 2–3, 1990, pp. 116–124.

[16]Martin, J. E., "Numerical Investigation of Three-Dimensionally Evolving Jets," Ph.D. Dissertation, Div. of Applied Mathematics, Brown Univ., Providence, RI, May 1991.

[17]Long, T. A., and Petersen, R. A., "Controlled Interactions in a Forced Axisymmetric Jet. Part 1. The Distortion of the Mean Flow," *Journal of Fluid Mechanics*, Vol. 235, 1992, pp. 37–55.

[18]Corke, T. C., and Kusek, S. M., "Resonance in Axisymmetric Jets with Controlled Helical-Mode Input," *Journal of Fluid Mechanics*, Vol. 249, 1993, pp. 307–336.

[19]Cho, S. K., "Vortex Pairing in an Axisymmetric Jet Using Acoustic Forcings," Ph.D. Dissertation, Dept. of Mechanical Engineering, Seoul National Univ., Seoul, Republic of Korea, Feb. 1998.

[20]Hajj, M. R., Miksad, R. W., and Powers, E. J., "Fundamental-Subharmonic Interaction: Effect of Phase Relation," *Journal of Fluid Mechanics*, Vol. 256, 1993, pp. 403–426.

[21]Yavuzkurt, S., "A Guide to Uncertainty Analysis of Hot-Wire Data," *Journal of Fluids Engineering*, Vol. 106, No. 2, 1984, pp. 181–186.

[22]Broze, G., and Hussain, F., "Nonlinear Dynamics of Forced Transitional Jets: Periodic and Chaotic Attractors," *Journal of Fluid Mechanics*, Vol. 263, 1994, pp. 93–132.

[23]Monkewitz, P. A., "Subharmonic Resonance, Pairing and Shredding in the Mixing Layer," *Journal of Fluid Mechanics*, Vol. 188, 1988, pp. 223–252.

[24]Broze, G., and Hussain, F., "Transitions to Chaos in a Forced Jet: Intermittency, Tangent Bifurcations and Hysterisis," *Journal of Fluid Mechanics*, Vol. 311, 1996, pp. 37–71.

J. C. Hermanson
Associate Editor